https://doi.org/10.5194/tc-2019-69
Preprint. Discussion started: 12 June 2019

The Cryosphere Discussions
Open Access
EGU

Influence of Sea Ice Anomalies on Antarctic Precipitation Using Source Attribution

Hailong Wang[1*], Jeremy Fyke[2,3], Jan Lenaerts[4], Jesse Nusbaumer[5,6], Hansi Singh[1], David Noone[7], and Philip Rasch[1]

(1) Pacific Northwest National Laboratory, Richland, WA

(2) Los Alamos National Laboratory, Los Alamos, NM

(3) Associated Engineering, Vernon, British Columbia, Canada

(4) Department of Atmospheric and Oceanic Sciences, University of Colorado at Boulder, Boulder, CO

(5) NASA Goddard Institute for Space Studies, New York, NY

(6) Center for Climate Systems Research, Columbia University, New York, NY

(7) Oregon State University, Corvallis, OR

[*]Correspondence to: Hailong.Wang@pnnl.gov

https://doi.org/10.5194/tc-2019-69
Preprint. Discussion started: 12 June 2019

Abstract

We conduct sensitivity experiments using a climate model that has an explicit water source tagging capability forced by prescribed composites of sea ice concentrations (SIC) and corresponding SSTs to understand the impact of sea ice anomalies on regional evaporation, moisture transport, and source–receptor relationships for precipitation over Antarctica. Surface sensible heat fluxes, evaporation, and column-integrated water vapor are larger over Southern Ocean (SO) areas with lower SIC, but changes in Antarctic precipitation and its source attribution with SICs reflect a strong spatial variability. Among the tagged source regions, the Southern Ocean (south of 50°S) contributes the most (40%) to the Antarctic total precipitation, followed by more northerly ocean basins, most notably the S. Pacific Ocean (27%), S. Indian Ocean (16%) and S. Atlantic Ocean (11%). The annual mean Antarctic precipitation is about 150 Gt/year more in the "low" SIC case than in the "high" SIC case. This difference is larger than the model-simulated interannual variability of Antarctic precipitation (99 Gt/year). The contrast in contribution from the S. Ocean, 102 Gt/year, is even more significant, compared to the interannual variability of 35 Gt/year in Antarctic precipitation that originates from the S. Ocean. The horizontal transport pathways from individual vapor source regions to Antarctica are largely determined by large-scale atmospheric circulation patterns. Vapor from lower latitude source regions takes elevated pathways to Antarctica. In contrast, vapor from the Southern Ocean moves southward within the lower troposphere to the Antarctic continent, so the contribution of nearby sources also depends on regional coastal topography. The impact of sea ice anomalies on regional Antarctic precipitation also depends on atmospheric circulation changes that result from the prescribed composite SIC/SST perturbations. In particular, regional wind anomalies along with surface evaporation changes determine regional shifts in the zonal and meridional moisture fluxes that can explain some of the resultant precipitation changes.

https://doi.org/10.5194/tc-2019-69
Preprint. Discussion started: 12 June 2019

1. Introduction

Antarctic surface mass balance (SMB) plays a critical role in determining the evolution of the Antarctic Ice Sheet (AIS) by supplying the vast majority of the positive mass component of the overall AIS mass balance (e.g., Lenaerts et al., 2012) through precipitation as snow. Variations of AIS SMB, dominated by changes in this precipitation (and to a lesser degree by sublimation), have profound implications for global mean sea level change. Modeling and experimental evidence suggests that AIS SMB increases in a warming climate due to increased precipitation as snowfall (e.g., Frieler et al., 2015; Grieger et al., 2016; Lenaerts et al., 2016; Zwally et al., 2015; Medley and Thomas, 2019). This SMB increase has the potential to offset a significant portion of the overall AIS mass loss due to ocean-driven mass loss (e.g., Winkelmann et al., 2012). However, the exact coupled-climate mechanisms driving this increase have not been well elucidated. In particular, the role of sea surface temperature (SST) changes, atmospheric moisture sources/transport/carrying capacity, sea ice loss, and atmospheric dynamical changes on Antarctic snowfall changes has not been clearly disaggregated. Observations and modeling have shown strongly heterogeneous spatial patterns and temporal variability in AIS SMB and its trends (e.g., Thomas et al., 2017; Lenaerts et al., 2018; Medley and Thomas, 2019), suggesting the presence of regional precipitation variability over AIS, which has been confirmed by previous studies using reanalysis and observational data (e.g., Bromwich et al., 2011; Behrangi et al., 2016; Palerme et al., 2017). Because of the extremely low local atmospheric moisture content, Antarctic precipitation relies on moisture transport from the surrounding oceans (e.g., Tietäväinen and Vihma, 2008). By analyzing long quasi-equilibrium global climate model simulations, Fyke et al. (2017) identified statistically significant relationships in Antarctic basin-scale precipitation patterns that are driven by variability in large-scale atmospheric moisture transport. However, the origin of moisture (i.e., evaporation source) and the impact of sea ice anomalies in the Southern Ocean on moisture source availability remain unclear.

Much of the Southern Ocean is seasonally covered by sea ice. Oceanic areas close to the Antarctic coast are ice-covered most of the year, but the sea ice pack can break up by strong winds originating from the ice sheet, generating coastal polynyas that expose open ocean to the atmosphere. Variations in sea ice cover and/or the polynyas not only affect local surface heat and moisture fluxes from the ocean (e.g., Weijer et al., 2017) but also shift the latitudes of the mid-latitude storm track (e.g., Kidston et al., 2011). In contrast to the Arctic sea ice loss observed in recent decades, sea ice cover in the Antarctic (Southern Ocean) has increased over the last few decades (Turner and Overland, 2009), followed by a strong decline from 2016 (https://nsidc.org/data). Coupled climate models that are able to reproduce the Arctic sea ice trends have difficulties simulating the increasing trend of sea ice cover in the Southern Ocean (e.g., Holland and Raphael, 2006; Meehl et al., 2016; Turner et al., 2013a). It is still unclear whether this trend

https://doi.org/10.5194/tc-2019-69
Preprint. Discussion started: 12 June 2019

in the Southern Ocean is due to natural or internal climate variability, and there is no convincing mechanistic explanation for such responses of the high-latitude climate system to the warming caused by anthropogenic forcing. Given potential connections between sea ice and Antarctic precipitation, this suggests a corresponding uncertainty in the projection of future precipitation changes over Antarctica (Agosta et al., 2015; Bracegirdle et al., 2015) and, by consequence, AIS SMB and global sea level rise. Understanding the impact of such sea ice anomalies on AIS SMB therefore presents an important scientific challenge (e.g., Kennicutt et al., 2015).

Moisture contributions from different source regions to local Antarctic precipitation cannot be quantified from direct measurements. Indirect approaches have to be used to derive such source–receptor relationships, characterize moisture history, and/or identify precipitation origins. Air parcel back-trajectory approaches tend to attribute more vapor sources to the high-latitude regions in the Southern Ocean (e.g., Helsen et al., 2007), likely due to the use of relatively short backward trajectories, which cannot trace water vapor originating from the distant low latitudes. A longer tracking time (e.g., 20 days) allows for the identification of more distant moisture sources of Antarctic precipitation that are generally consistent with isotope-based source reconstruction and general circulation model (GCM) results (Sodemann and Stohl, 2009). However, for tracking times beyond 10 days, trajectory calculation error can become unacceptably large due to the reduced coherency of air parcels (Sodemann et al., 2008). Atmospheric GCMs with moisture tracking capability using water isotope or tagged water tracers provide a powerful means to determine the origin of moisture sources of precipitation over receptor regions such as Antarctica (e.g., Koster et al., 1986; Delaygue et al., 2000; Noone and Simmonds, 2002; Singh et al., 2016a). Such studies have shown that moisture sources for precipitation over the AIS are primarily from the Southern Ocean (south of 50°S) and the Southern Hemisphere mid-latitude oceans.

In this study, we aim to understand the impact of Southern Ocean sea ice anomalies on local evaporation, moisture transport and source–receptor relationships for moisture and precipitation over Antarctica using a GCM that has an explicit water source tagging capability. Section 2 describes the GCM with water tagging capability and the experimental design. Main results and related discussions are presented in Section 3. Section 4 summarizes key conclusions drawn from these sensitivity experiments and water source attribution analysis.

2. Methodology

2.1 Model description

https://doi.org/10.5194/tc-2019-69
Preprint. Discussion started: 12 June 2019

The climate model employed in this study is a coupled atmosphere-land version of the Community Earth System Model (CESM1-CAM5, CESM hereafter; Hurrell et al., 2013) that has an atmospheric water tagging capability (e.g., Singh et al., 2016a; Singh et al., 2016b; Singh et al., 2017; Nusbaumer and Noone, 2018; Tabor et al., 2018). The atmospheric component, called the Community Atmosphere Model version 5 (CAM5), can also be run with prescribed sea surface temperature (SST) and sea ice concentrations (SICs) coupled with an interactive land component (CLM4, Oleson et al., 2010), which includes the evolution of ice and snow over land. Sea ice thickness and snow cover over sea ice still evolve in the model, although SSTs and SICs are prescribed. CAM5 has relatively comprehensive representations of surface evaporation, clouds, precipitation, and atmospheric circulation (Neale et al., 2010).

The atmospheric water tagging capability in CAM5 can be used to track water that enters the atmosphere through surface evaporation in any given region, moves with the air mass, condenses into liquid or ice clouds, and forms precipitation (rain or snow). A set of new water variables (designated as a tagged water tracer set) is defined in CAM5 to capture the mass mixing ratio of vapor, cloud liquid, cloud ice, stratiform rain, stratiform snow, convective rain, and convective snow for each water source region of interest. Each water tracer set undergoes the same atmospheric processes as the corresponding standard water variables in the model. The tracked water cycle starts with surface evaporation/sublimation and ends when water returns to the Earth's surface in the form of condensate or precipitation. Thus the destiny of the tracer water is lost once it returns to the surface.

2.2 Experimental design

We use the water tagging capability along with a set of sensitivity experiments to examine the impact of changes in sea ice concentration (SIC) in the Southern Ocean on moisture transport, Antarctic snowfall, and the AIS SMB. Here SIC is defined as the fractional area of ocean in a model grid that is covered by sea ice. Three SIC (and corresponding SST) composites are constructed from the pre-industrial control simulation of the CESM large ensemble (Kay et al., 2015), which gives a continuous time series of over 1000 years to perform our composite analysis of SIC and SST. A baseline simulation uses the mean SIC/SST distributions and two sensitivity simulations use the 10% lowest and highest annual average total Southern Hemisphere SIC, respectively, coupled to the corresponding anomalies in global SSTs. All other forcing conditions (e.g., solar, greenhouse gases, anthropogenic aerosols) are identical across simulations.

https://doi.org/10.5194/tc-2019-69
Preprint. Discussion started: 12 June 2019

The three simulations (hereafter referred to as "mean", "low" and "high" according to the prescribed SICs) are conducted at a horizontal grid spacing of 0.9° × 1.25° with 30 vertical levels for 11 years. Results from the last 10 years are analyzed, assuming that the first simulation year is for model spin up. Figure 1 shows the anomalies of the two SIC composites with respect to the annual and seasonal mean SIC. The most widespread SIC anomalies are found in the Weddell sea and the Bellingshausen and Amundsen seas in the austral autumn (MAM) and summer (DJF). The largest reduction in the "low" SIC case is along the east coast of the Antarctic Peninsula in MAM and DJF, while the most positive anomalies in the "high" SIC case are in the Amundsen sea further away from the coastal zone in JJA and SON. SIC anomalies are relatively small in the eastern Antarctic/SO sectors where the mean sea ice extent and SIC are also smaller. The regional difference in SIC anomalies adapted from the CESM LENS simulations is likely related to the key role of the Amundsen-Bellingshausen Seas Low (ABSL) in controlling the regional climate variability (e.g., Hosking et al., 2013). The magnitude and location of prescribed SIC anomalies are comparable to the observed SIC changes during the recent decades (Hobbs et al., 2016).

To use the water tracer tagging capability of CESM, we need to predefine water vapor source regions, where surface evaporation/sublimation of water provides the initial source of water vapor entering the atmospheric hydrologic cycle for the corresponding source region tags. Figure 2 shows global annual mean evaporation/sublimation rate from the "mean" SIC case and the water source regions, including major tropical, subtropical and mid-latitude ocean basins, land (all continents) and several finer sectors in the Southern Ocean (SO), that are tagged in all three simulations. According to Singh et al. (2017), the more distant lower-latitude oceans (i.e., 30°S equatorward) are much less efficient in contributing to Antarctic precipitation, and there is no seasonal sea ice over in the lower-latitude oceans, so each of these tags is set up to cover a quite large area to economize computing time. Much finer divisions are used for the SO because they are in close proximity to the Antarctic and their surface evaporation is more affected by SIC variations. Five regular latitude-longitude boxes are well defined. The remaining area (irregular shape) of the SO was constructed by differencing between the entire S. Ocean tag and the sum of the five regular regions.

3. Results and Discussions

3.1 Responses of surface fluxes, precipitable water and precipitation to the SIC and SST anomalies

Although the three SIC composites were based on annual mean sea ice data, there are also large and consistent seasonal differences in SIC prescribed in the 'low' and 'high' sea ice cases (Fig. 1). The most widespread differences are in the Weddell Sea and the King Haakon VII Sea where the reduction in "low"

https://doi.org/10.5194/tc-2019-69
Preprint. Discussion started: 12 June 2019

SIC extends north of 60°S, while the largest difference (over 20%) occurs in the Bellingshausen Sea and the Amundsen Sea (Fig. 3a), indicating the role of ABSL in dominating the overall interannual variability of sea ice cover in the Southern Ocean. Compared to the "high" SIC case, the "low" SIC case also has much warmer mean SST and higher surface sensible heat flux and evaporation over the lower SIC areas (Figs. 3b, d and e). The sensible heat flux and evaporation over the northern latitudes of the SO also show large differences between the two cases, likely due to meteorological responses (e.g., changes in wind, temperature, and humidity) to the SIC/SST differences. The total precipitable water (PW) in the low SIC case is greater over most of the SO, while the precipitation is greater over most of the coastal areas except for the King Haakon VII Sea (Fig. 3c and f). The coastal area that has less precipitation in the low SIC case, mostly occurring in austral winter (JJA) when SIC near coastal regions is almost the same in the two cases (Fig. 1), is characterized by anomalous meridional moisture divergence (figure not shown), echoing the finding of Fyke et al. (2017).

3.2 Seasonal variation of Antarctic precipitation and source attribution

As expected, there are strong seasonal variations in total Antarctic precipitation, and a distinct minimum in austral summer months (Fig. 4), which is opposite to the PW seasonal cycle (Fig. S1). Although the seasonal pattern itself changes very little with the SIC/SST anomalies, the magnitude of seasonal precipitation has relatively larger changes, as well as larger interannual variability (indicated by the longer error bars), in spring and fall than the other months, which is consistent with SIC changes between the "low" and "high" cases (Fig. 1). The annual mean precipitation is about 150 Gt/year more in the "low" SIC case than in the "high" SIC case, representing a 6% increase relative to the total precipitation (2500 Gt/year) in the "mean" SIC case. This difference is larger than the interannual variability of Antarctic precipitation (99 Gt/year) that is characterized by one standard deviation of annual mean precipitation within the 10 years of the "mean" SIC case. Note that the standard deviation of annual mean Antarctic precipitation for the entire CESM LENS time series is 98 Gt/year, which is smaller than the variability of 122 Gt/year for recent historical precipitation simulated in CESM (Fyke et al., 2017). The contrast in precipitation between the "low" and "high" SIC cases contributed by the S. Ocean, 102 Gt/year, is more significant, compared to the interannual variability of 35 Gt/year in precipitation that originates from the S. Ocean, although it is a small fraction of the increase in evaporation (870 Gt/year) from the S. Ocean (again comparing the "low" SIC case to the "high" SIC case).

Among the tagged source regions, the S. Ocean (including the 6 sub-sectors) contributes the most (40%) to the Antarctic total precipitation in the "mean" SIC case, followed by S. Pacific Ocean (27%), S. Indian Ocean (16%) and S. Atlantic Ocean (11%), with the remaining mostly coming from

https://doi.org/10.5194/tc-2019-69
Preprint. Discussion started: 12 June 2019

evaporation/sublimation over land. The other oceans in the tropics and northern hemisphere have a negligible contribution to Antarctic moisture and precipitation. The fractional contribution by S. Ocean has a 1.7% increase (comparing the "low" SIC case to the "high" SIC case), while there is a small decrease from S. Atlantic (-0.7%) and S. Pacific (-1%). The contribution by S. Ocean, Land and some remote oceans (e.g., S. Indian Ocean and S. Pacific Ocean) has a relatively strong seasonal variation. There is a seasonal peak contribution from the S. Ocean in fall and spring (MAM and SON), when the SIC anomalies make a relatively large difference to the total Antarctic precipitation (Fig. 4), while the peak is in boreal summer (JJA) for the remote oceans and in austral summer (DJF) for land sources. The annual mean contribution of 40% by S. Ocean is larger than the estimate (30%) by Sodemann and Stohl (2009) using the 20-day back trajectory method. Also different from the finding of Sodemann and Stohl (2009), the seasonal cycle of the S. Ocean contribution to Antarctic precipitation in our study is not mainly determined by the SIC seasonality.

As shown in Fig. (3f), SIC/SST-driven changes in Antarctic precipitation have a strong spatial variability, as does the source attribution. Figure 5 shows the spatial distribution of fractional contributions by individual and combined source tags. The five major source regions together account for over 95% of total Antarctic precipitation, with individual regions dominating in certain areas as determined by geographical location and atmospheric circulation patterns. The S. Ocean tag as a whole dominates precipitation over most of the coastal areas except for the segment (90–150°E) located at the south of the S. India Ocean. The sub-sector sources in the SO primarily affect nearby coastal areas as well as downwind coastal and inland regions. There is also a strong regional variation in the changes of absolute precipitation and corresponding fractional contribution from individual source regions related to the SIC anomalies (Figs. S2 and S3). The higher fractional contribution in the lower SIC case from the S. Ocean and sub-sectors is mostly due to increased coastal precipitation, while changes in the fractional contribution by more remote sources do not correspond well with the absolute precipitation change over the SO and Antarctica. This arises because small changes in precipitation originating from remote sources can be overwhelmed by large changes from local sources. Such compensating effects occur not only between the local source region (S. Ocean) and remote source regions but also amongst the remote region contributions themselves.

To further look at spatial variations in precipitation and its source attribution, we divide Antarctica into three broad sectors: eastern Antarctica (0, 180°E; 65°S, 80°S), western Antarctica (0, 180°W; 65°S, 80°S), and interior Antarctica (80°S, 90°S). The contribution of the entire S. Ocean source tag to the annual mean precipitation dominates over all three and has a small interannual variation, although seasonal variations of contribution have large differences (Fig. S4). The S. Ocean has a larger

https://doi.org/10.5194/tc-2019-69
Preprint. Discussion started: 12 June 2019

contribution to precipitation over western Antarctica than eastern Antarctica, which is in part due to higher elevation in the east. Among the major remote source regions, the S. Indian Ocean and S. Atlantic dominate the contribution to precipitation over eastern Antarctica, while the S. Pacific Ocean dominates over western and interior Antarctica, especially in austral winter (JJA).

3.3 Transport pathways of water to Antarctica

As shown in previous studies (e.g., Wang et al., 2014; Singh et al., 2017), as well as indicated in the previous section (Fig. 5), the horizontal transport pathways of atmospheric constituents such as vapor and aerosol particles from individual source regions to a receptor are largely determined by large-scale atmospheric circulations. Localized or large-scale vertical lifting at the source region is an important factor in determining the extent to which this vapor can penetrate to the Antarctic interior before precipitating. Figure 6 shows the vertical distribution of fractional contribution to zonal mean water vapor mixing ratio by the major source regions for Antarctic precipitation. In general, vapor originating from remote source regions at lower latitudes and northern hemisphere takes elevated pathways to Antarctica while vapor from the nearby tags in the SO moves southward within the lower troposphere, as noted in previous studies (e.g., Noone and Simmonds, 2002; Sodemann and Stohl, 2009). The meridional and vertical transport of vapor is along zonal mean moist isentropes moist (θ_e) that are largely shaped by local topography in Antarctica (Fig. S5). As a result, a large portion (up to 70% for the zonal mean) of the vapor below 700 mb comes from the S. Ocean source tag, which also contributes a significant amount (10-40%) to vapor in the mid-troposphere (700–400 mb). Vapor in the upper troposphere (above 400 mb) predominantly comes from remote oceans through elevated pathways, although evaporation from lower-latitude continents also contribute at a discernible fraction (up to 20%). Vapor originating from the equatorial oceans, lifted by deep convection in the ITCZ, can have a substantial contribution (up to 40%) at very high levels (above 200 mb).

Clouds over Antarctica are dominated by the ice phase or mixed phase (containing supercooled liquid), especially at high altitudes (above 600 mb). Figure 7 shows the vertical distribution of fractional contributions to zonal mean ice water mixing ratio by the major source regions. It is generally consistent with that for water vapor but with differences in the magnitude and spatial patterns, presumably, due to different cloud-formation mechanisms. For instance, the large contribution by the S. Ocean tag between 50°S and 70°S are related to Southern Ocean storm dynamics and the strong orographic lifting of local moisture. The contribution by remote sources in the middle and upper troposphere is more likely determined by large-scale dynamics and local ambient conditions.

We have shown in the previous section that the SO SIC reduction substantially increases the atmospheric column-integrated water vapor. The increase is mostly in the lower troposphere over the SO and coastal

https://doi.org/10.5194/tc-2019-69
Preprint. Discussion started: 12 June 2019

areas (Fig. 8), where water vapor sources include the S. Pacific, S. Indian Ocean and S. Atlantic in addition to the primary contributor, S. Ocean (Fig. 6). However, the three remote source regions contribute less water vapor further inland in the "low" SIC case (Fig. 8), which leads to a discernable reduction in their fractional contribution to water vapor in the lower and mid troposphere (Fig. 9). As expected, the contribution by the entire S. Ocean tag increases substantially south of 50°S in the "low" SIC case, compensating for the reduced contribution from remote oceans. Note that the changes in fractional contribution in the upper troposphere and lower stratosphere (Fig. 9) are more likely related to SST and deep convection changes in the lower latitudes than to the SIC changes.

3.4 Changes in meridional transport and circulation patterns

SIC changes between the "low" and "high" cases can be closely associated with large-scale circulation changes over the SO. Previous studies identified complex large-scale interactions between the atmosphere and Antarctic sea ice cover, which are dependent on sub-sectors in the SO (e.g., Lefebvre and Goose, 2008; Hobbs et al., 2016). Meridional winds can drive the exchange of dry/cold air over the AIS with moist/warm air from lower-latitude oceans. Moisture from the north moves to Antarctica over the entire SO (not shown) and outflow (southerly wind) associated with the polar high brings relatively dry air back to the ocean. Along with the SIC difference between the "low" and "high" cases, the meridional moisture flux that is largely determined by meridional winds also changes (Fig. 10a). Changes in meridional wind can be explained by the sea level pressure change using the geostrophic balance approximation, especially in JJA (Fig. 10c). The pattern of variations in meridional moisture flux is also correlated with precipitation differences (Fig. 3f). As a result, decreases in precipitation in the "low" SIC case over the King Haakon VII Sea and Wilkes Land sector can be traced to a SIC-caused reduction in meridional flow and related moisture fluxes from the north (Fig.10a). Although the experimental design in this study doesn't allow us to pinpoint a causal relationship among the three effects (i.e., lower SIC, reduced meridional moisture flux, and precipitation decrease), large-scale moisture transport has been identified as the main driver of basin-scale precipitation variations over Antarctica (e.g., Fyke et al., 2017). The reduced moisture influx is expected to cause a decrease in vapor and precipitation in those areas. Since a lower SIC corresponds to a stronger local evaporation at the surface, the reduction in moisture flux coming from the mid-latitude ocean is more likely due to the weaker meridional flow (Fig. 10c). Therefore, the impact of sea ice anomalies and corresponding SST changes on Antarctic precipitation stem both from their direct impact on moisture sources and from the circulation changes that accompany the different SIC and SST patterns.

Comparison between the "low" and "high" cases also shows a strengthening of the Hadley Cell and weakening of the polar vortex in the southern hemisphere accompanying the "low" SIC (figure not

https://doi.org/10.5194/tc-2019-69
Preprint. Discussion started: 12 June 2019

shown). Variations in zonal flow and moisture fluxes over much of the SO (Fig. 10b, d) can affect Antarctic precipitation through redistribution of moisture among the different sectors/basins and indirect changes in northward moisture transport. Regional westerlies can also drive changes in upper-ocean heat storage and sea ice formation by affecting Ekman pumping and thus the sea ice extent (e.g., Turner et al., 2013b). The southern annular mode, which dominates the variability of the large-scale atmospheric circulation in the Southern Hemisphere, has been found to co-vary with tropical SST variability (e.g., Ding et al., 2012) and respond to SIC changes (e.g., Menéndez et al., 1999; Bader et al., 2013; Smith et al., 2017). The Amundsen-Bellingshausen Seas Low (ABSL), which plays an important role in bringing warm/moist air into the Bellingshausen Sea and Antarctic Peninsula region and moving cold/dry air equatorward through the Ross Sea region, strongly influences winds, near-surface temperature, precipitation and SIC over the Amundsen-Bellingshausen Seas (e.g., Hosking et al., 2013). Conversely, the strength and location of the ABSL can also be affected by the sea ice and temperature changes, as depicted in Fig. 10e. Therefore, such changes in the atmospheric circulations related to the SIC/SST anomalies are likely to influence regional precipitation over Antarctica. Here we do not elaborate on causes of CESM-simulated SO SIC/SST anomalies in the Large Ensemble that promulgate the resulting circulation changes when prescribed in our sensitivity experiments.

4. Summary and Conclusions

In this study, we use a coupled atmosphere-land version of the Community Earth System Model (CESM1-CAM5) with explicit water tagging capability to quantify the impact of sea surface temperature (SST) and sea ice concentration (SIC) changes on the moisture sources of Antarctic precipitation. A set of sensitivity experiments are conducted to understand the impact of SIC and SST variations on regional evaporation, moisture transport, and source–receptor relationships for Antarctic precipitation. Three composites of sea ice concentrations (SIC), which were constructed from the 1800-year fully-coupled control simulation of the CESM Large Ensemble Project using mean, 10% lowest, and 10% highest SIC years (and corresponding SSTs), respectively, are used as prescribed boundary conditions for atmosphere-only simulations. Moisture originating from individual geographical regions is explicitly tracked using separate water tracers throughout the atmospheric water cycle that closes with surface precipitation.

Because of the prescribed changes in the SIC and SST, surface sensible heat fluxes and evaporation over the lower SIC areas in the Southern Ocean (SO) have a large increase in the “low” SIC case, compared to the “high” SIC case. Column-integrated water vapor also increases over much of the SO, while changes in Antarctic precipitation with SICs have a strong spatial variability, as does the source attribution. Among the tagged source regions, the S. Ocean (including all six sub-sectors) contributes the most (40%) to the

https://doi.org/10.5194/tc-2019-69
Preprint. Discussion started: 12 June 2019

Antarctic total precipitation, followed by S. Pacific Ocean (27%), S. Indian Ocean (16%) and S. Atlantic Ocean (11%), with the remaining contributions mostly from evaporation or sublimation over global land. The three remote source regions have a reduced absolute contribution to water vapor further inland in the "low" SIC case, which leads to a discernable reduction in their fractional contribution, especially, in the lower and mid troposphere. With lower SIC, the relative contribution to water vapor south of 50°S by the S. Ocean tag increases substantially, compensating the reduction in the relative contribution from remote oceans. This is qualitatively consistent with the source attribution change in response to warming from CO_2 doubling (Singh et al., 2017). The annual mean total Antarctic precipitation is approximately 150 Gt/year more in the "low" SIC case than in the "high" SIC case. This difference is larger than the interannual variability of Antarctic precipitation (characterized by one standard deviation of annual mean precipitation) within the 10 years of the "mean" SIC case as well as over 1000 years of the CESM LENS experiment. The contrast in precipitation between the "low" and "high" SIC cases contributed by the S. Ocean, 102 Gt/year, is even more significant, compared to the interannual variability of 35 Gt/year in precipitation that originates from the S. Ocean.

The horizontal transport pathways from individual vapor source regions to Antarctica are largely determined by large-scale atmospheric circulations. Localized or large-scale vertical lifting is important in determining the heights at which vapor is transported. Thus the source contribution is primarily determined by their geographical location (and atmospheric dynamical setting) and atmospheric circulation patterns, as well as the local elevation over Antarctica. Vapor from source regions at lower latitudes takes elevated pathways to Antarctica while vapor from the nearby tags in the SO moves southward within the lower troposphere. The entire S. Ocean source tag is the primary contributor to the annual mean precipitation over all defined Antarctic sub-regions - eastern Antarctica (0, 180°E; 65°S, 80°S), western Antarctica (0, 180°W; 65°S, 80°S), and interior Antarctica (80°S, 90°S). However, it has a larger contribution to precipitation over western Antarctica than eastern Antarctica, which is in part due to higher elevation in the east. The S. Ocean contribution also has large seasonal differences among the three. Among the remote source regions, S. Indian Ocean and S. Atlantic dominate the contribution to precipitation over eastern Antarctica, while S. Pacific Ocean dominates over western and interior Antarctica, especially in austral winter (JJA).

In addition to direct thermodynamic effects, the impact of sea ice anomalies on regional precipitation over Antarctica also depends on atmospheric circulation changes that result from the SIC/SST perturbations prescribed to the simulations. Regional anomalies in zonal and meridional winds combine with surface evaporation changes to determine regional shifts in zonal and meridional moisture fluxes. The resultant changes in meridional moisture fluxes from the Southern Ocean to the Antarctic continent can intuitively

https://doi.org/10.5194/tc-2019-69
Preprint. Discussion started: 12 June 2019

explain some of the precipitation differences between the "low" and "high" SIC cases. Variations in zonal moisture fluxes can also potentially affect Antarctic precipitation indirectly through the redistribution of moisture among the different sectors/basins. However, the experiment design of this study doesn't allow us to isolate the impact of SIC anomalies on circulation-driven changes in Antarctic precipitation. A future study with specified large-scale circulations might be helpful in this regard.

Code and data availability. The CESM model code can be obtained from http://www.cesm.ucar.edu/ and https://github.com/CESM-Development. Directions for obtaining CESM Large Ensemble data are available at www.cesm.ucar.edu/projects/community-projects/LENS/. The model simulations will be made available upon request to the corresponding author.

Competing interests. The authors declare that they have no conflict of interest.

Acknowledgments. This research is based on work supported by the U.S. Department of Energy (DOE), Office of Science, Biological and Environmental Research as part of the Regional and Global Model Analysis (RGMA) program. Jan T. M. Lenaerts acknowledges support from the National Aeronautics and Space Administration (NASA) through project 80NSSC18K1025. Jesse Nusbaumer was supported by the NASA Post-doctoral Program (NPP) fellowship. The Pacific Northwest National Laboratory (PNNL) is operated for DOE by Battelle Memorial Institute under contract DE-AC05-76RLO1830. The CESM project is supported by the National Science Foundation and the DOE Office of Science. We would like to acknowledge high-performance computing support from Yellowstone (ark:/85065/d7wd3xhc) provided by NCAR's Computational and Information Systems Laboratory, sponsored by the National Science Foundation.

References

Agosta, C., Fettweis, X., and Datta, R.: Evaluation of the CMIP5 models in the aim of regional modelling of the Antarctic surface mass balance, The Cryosphere, 9, 2311-2321, https://doi.org/10.5194/tc-9-2311-2015, 2015.

Bader, J., Flügge, M., Kvamstø, N. G., Mesquita, M. D. S., and A. Voigt, A.: Atmospheric winter response to a projected future Antarctic sea-ice reduction: A dynamical analysis. Climate Dyn., 40, 2707–2718, doi:https://doi.org/10.1007/s00382-012-1507-9, 2013.

Behrangi, A., Christensen, M., Richardson, M., Lebsock, M., Stephens, G., Huffman, G. J., Bolvin, D., Adler, R. F., Gardner, A., Lambrigtsen, B., and Fetzer, E.: Status of high-latitude precipitation

https://doi.org/10.5194/tc-2019-69
Preprint. Discussion started: 12 June 2019

estimates from observations and reanalyses, J. Geophys. Res. Atmos., 121, 4468– 4486, doi:10.1002/2015JD024546, 2016.

Bracegirdle, T. J., Stephenson, D. B., Turner, J., and Phillips, T.: The importance of sea ice area biases in 21st century multimodel projections of Antarctic temperature and precipitation. Geophys. Res. Lett. 42, 10,832–810,839, 2015.

Bromwich, D. H., Nicolas, J. P., and Monaghan, A. J.: An Assessment of Precipitation Changes over Antarctica and the Southern Ocean since 1989 in Contemporary Global Reanalyses. J. Climate, 24, 4189–4209, https://doi.org/10.1175/2011JCLI4074.1, 2011.

Delaygue, G., Masson, V., Jouzel, J., Koster, R. D., and Healy, R. J.: The origin of Antarctic precipitation: A modelling approach, Tellus, Ser. B, 52, 19– 36, 2000.

Ding, Q., Steig, E. J., Battisti, D. S., and Wallace, J. M.: Influence of the Tropics on the Southern Annular Mode. J. Climate, 25, 6330–6348, https://doi.org/10.1175/JCLI-D-11-00523.1, 2012.

Frieler, K., Clark, P. U., He, F., Buizert, C., Reese, R., Ligtenberg, S. R. M., van den Broeke, M. R., Winkelmann, R., and Levermann, A.: Consistent evidence of increasing Antarctic accumulation with warming, Nature Climate Change, 5, 348–352, https://doi.org/10.1038/nclimate2574, 2015.

Fyke, J., Lenaerts, J., and Wang, H.: Basin-scale heterogeneity in Antarctic precipitation and its impact on surface mass variability. The Cryosphere, 11(6), 2595-2609, 2017.

Grieger, J., Leckebusch, G.C. and Ulbrich, U.: Net precipitation of Antarctica: thermodynamical and dynamical parts of the climate change signal. Journal of Climate, 29, 907-924, 2016.

Helsen, M. M., van de Wal, R. S. W., and den Broeke, M. R. V.: The isotopic composition of present-day Antarctic snow in a Lagrangian atmospheric simulation, J. Clim., 20, 739– 756, 2007.

Hobbs, W.R., Massom, R., Stammerjohn, S., Reid, P., Williams, G. and Meier, W., 2016. A review of recent changes in Southern Ocean sea ice, their drivers and forcings. Global and Planetary Change, 143, 228-250, 2016.

Holland, M. and Raphael, M.: Twentieth century simulation of the southern hemisphere climate in coupled models, Part II: sea ice conditions and variability, Clim. Dynam., 26, 229–245, doi:10.1007/s00382-005-0087-3, 2006.

Hosking, J.S., Orr, A., Marshall, G.J., Turner, J., and Phillips, T.: The influence of the Amundsen–Bellingshausen Seas Low on the climate of West Antarctica and its representation in coupled climate model simulations. J. Climate, 26, 6633–6648, https://doi.org/10.1175/JCLI-D-12-00813.1, 2013.

Kay, J. E., Deser, C., Phillips, A., Mai, A., Hannay, C., Strand, G., Arblaster, J. M., Bates, S. C., Danabasoglu, G., Edwards, J., Holland, M., Kushner, P., Lamarque, J.-F., Lawrence, D., Lindsay, K., Middleton, A., Munoz, E., Neale, R., Oleson, K., Polvani, L., and Vertenstein, M.: The Community Earth System Model (CESM) Large Ensemble Project: A Community Resource for Studying Climate

https://doi.org/10.5194/tc-2019-69
Preprint. Discussion started: 12 June 2019

Change in the Presence of Internal Climate Variability, B. Am. Meteorol. Soc., 96, 1333–1349, https://doi.org/10.1175/BAMS-D-13-00255.1, 2015.

Kennicutt, M.C., Chown, S.L., Cassano, J.J., Liggett, D., Peck, L.S., Massom, R., Rintoul, S.R., Storey, J., Vaughan, D.G., Wilson, T.J. and Allison, I.: A roadmap for Antarctic and Southern Ocean science for the next two decades and beyond. Antarctic Science, 27, 3–18. http://dx.doi.org/10.1017/S0954102014000674, 2015.

Kidston, J., Taschetto, A.S., Thompson, D.W.J., England, M.H.: The influence of Southern Hemisphere sea-ice extent on the latitude of the mid-latitude jet stream. Geophys. Res. Lett., 38, L15804, http://dx.doi.org/10.1029/2011gl048056, 2011.

Koster, R., Jouzel, J., Suozzo, R., Russell, G., Broecker, W., Rind, D., and Eagleson, P.: Global sources of local precipitation as determined by the NASA/GISS GCM. Geophysical Research Letters, 13, 121-124, 1986.

Lefebvre, W. and Goosse, H.: An analysis of the atmospheric processes driving the large-scale winter sea ice variability in the Southern Ocean, J. Geophys. Res., 113, doi:10.1029/2006JC004032, 2008.

Lenaerts, J.T.M., Van den Broeke, M.R., Van de Berg, W.J., Van Meijgaard, E., and Kuipers Munneke, P.: A new, high-resolution surface mass balance map of Antarctica (1979–2010) based on regional atmospheric climate modeling. Geophysical Research Letters, 39, L04501, doi:10.1029/2011GL050713, 2012.

Lenaerts, J. T. M., Vizcaino, M., Fyke, J., van Kampenhout, L., and van den Broeke, M. R.: Present-day and future Antarctic ice sheet climate and surface mass balance in the Community Earth System Model, Clim. Dynam., 47, 1–15, https://doi.org/10.1007/s00382-015-2907-4, 2016.

Lenaerts, J. T. M., Fyke, J., and Medley, B.: The signature of ozone depletion in recent Antarctic precipitation change: A study with the Community Earth System Model. Geophysical Research Letters, 45, 12,931–12,939. https://doi.org/10.1029/2018GL078608, 2018.

Medley, B., and Thomas, E. R.: Increased snowfall over the Antarctic Ice Sheet mitigated 20th century sea-level rise. Nature Climate Change, 9, 34-39. https://doi.org/10.1038/s41558-018-0356-x, 2019.

Meehl, G.A., Arblaster, J.M., Bitz, C.M., Chung, C.T. and Teng, H.: Antarctic sea-ice expansion between 2000 and 2014 driven by tropical Pacific decadal climate variability. Nature Geoscience, 9, 590–595. doi:10.1038/ngeo2751, 2016.

Menéndez, C. G., Serafini, V., and Le Treut, H., 1999: The effect of sea-ice on the transient atmospheric eddies of the Southern Hemisphere. Climate Dyn., 15, 659–671, 1999.

Neale, R.B., Chen, C.C., Gettelman, A., Lauritzen, P.H., Park, S., Williamson, D.L., Conley, A.J., Garcia, R., Kinnison, D., Lamarque, J.F. and Marsh, D.: Description of the NCAR community atmosphere model (CAM 5.0). NCAR Tech. Note TN-486, 274 pp, 2012.

https://doi.org/10.5194/tc-2019-69
Preprint. Discussion started: 12 June 2019

Noone, D. C., and Simmonds, I.: Annular variations in moisture transport mechanisms and the abundance of $\delta^{18}O$ in Antarctic snow, Journal of Geophysical Research: Atmosphere, 107(D24), 4742, doi:10.1029/2002JD002262, 2002.

Noone, D. C., and Simmonds, I.: Sea ice control of water isotope transport to Antarctica and implications for ice core interpretation, Journal of Geophysical Research: Atmospheres, 109, D7, 2004.

Nusbaumer, J., and Noone, D.C.: Numerical Evaluation of the Modern and Future Origins of Atmospheric River Moisture Over the West Coast of the United States, Journal of Geophysical Research: Atmospheres, 123(12), 6423-6442, doi: 10.1029/2017JD028081, 2018.

Oleson, K. W., Lawrence, D. M., Bonan, G. B., Flanner, M. G., Kluzek, E., Lawrence, P. J., Levis, S., Swenson, S. C., Thorn- ton, P. E., Dai, A., Decker, M., Dickinson, R., Feddema, J., Heald, C. L., Hoffman, F., Lamarque, J., Mahowald, N., Niu, G., Qian, T., Randerson, J., Running, S., Sakaguchi, K., Slater, A., Stockli, R., Wang, A., Yang, Z., Zeng, X., and Zeng, X.: Technical Description of version 4.0 of the Community Land Model (CLM), NCAR Technical Note NCAR/TN-478+STR, doi:10.5065/D6FB50WZ, 2010.

Palerme, C., Genthon, C., Claud, C., Kay, J. E., Wood, N. B., and L'Ecuyer, T.: Evaluation of current and projected Antarctic precipitation in CMIP5 models, Clim. Dynam., 48, 1–15, https://doi.org/10.1007/s00382-016-3071-1, 2016.

Singh, H. A., Bitz, C. M., Nusbaumer, J., and Noone, D. C.: A mathematical framework for analysis of water tracers: Part 1: Development of theory and application to the preindustrial mean state, J. Adv. Model. Earth Syst., 8, 991–1013, doi: 10.1002/2016MS000649, 2016a.

Singh, H. A., Bitz, C. M., Donohoe, A., Nusbaumer, J., and Noone, D. C.: A Mathematical Framework for Analysis of Water Tracers. Part II: Understanding Large-Scale Perturbations in the Hydrological Cycle due to CO_2 Doubling , J. Climate, 10.1175/JCLI-D-16-0293.1, 29, 6765-6782, 2016b.

Singh, H. A., Bitz, C. M., Donohoe, A., and Rasch, P. J.: A source–receptor perspective on the polar hydrologic cycle: Sources, seasonality, and Arctic–Antarctic parity in the hydrologic cycle response to CO_2 doubling, J. Climate, 30, 9999-10017, 2017.

Smith, D. M., Dunstone, N. J., Scaife, A. A., Fiedler, E. K., Copsey, D., and Hardiman, S. C.: Atmospheric response to Arctic and Antarctic sea ice: The importance of ocean–atmosphere coupling and the background state. J. Climate, 30, 4547–4565, https://doi.org/10.1175/JCLI-D-16-0564.1, 2017.

Sodemann, H., Schwierz, C., and Wernli, H.: Interannual variability of Greenland winter precipitation sources: Lagrangian moisture diagnostic and North Atlantic Oscillation influence, J. Geophys. Res., 113, D03107, doi:10.1029/2007JD008503, 2008.

Sodemann, H., and Stohl, A.: Asymmetries in the moisture origin of Antarctic precipitation. Geophys.

https://doi.org/10.5194/tc-2019-69
Preprint. Discussion started: 12 June 2019

Res. Lett., 36, L22803, doi:10.1029/2009GL040242, 2009.

Tabor, C., Otto-bliesner, B., Brady, E. C., Nusbaumer, J., Zhu, J., Erb, M. P., Wong, T. E., Liu, Z., and Noone, D. C.: Interpreting precession-driven $\delta^{18}O$ variability in the South Asian monsoon region, 123(11), 5927-5946, doi: 10.1029/2018JD028424., 2018.

Thomas, E. R., van Wessem, J. M., Roberts, J., Isaksson, E., Schlosser, E., Fudge, T. J., Vallelonga, P., Medley, B., Lenaerts, J., Bertler, N., van den Broeke, M. R., Dixon, D. A., Frezzotti, M., Stenni, B., Curran, M., and Ekaykin, A. A.: Regional Antarctic snow accumulation over the past 1000 years, Clim. Past, 13, 1491-1513, https://doi.org/10.5194/cp-13-1491-2017, 2017.

Tietäväinen, H., and Vihma, T.: Atmospheric moisture budget over Antarctica and the Southern Ocean based on the ERA-40 reanalysis. Int. J. Climatol., 28, 1977–1995, 2008.

Turner, J. and Overland, J.: Contrasting climate change in the two polar regions", Polar Research, 28, 146-164. doi:10.3402/polar.v28i2.6120, 2009.

Turner, J., Bracegirdle, T. J., Phillips, T., Marshall, G. J., Hosking, J. S.: An initial assessment of Antarctic sea ice extent in the CMIP5 models. J. Clim., 26, 1473–1484. http://dx.doi.org/10.1175/Jcli-D-12-00068.1, 2013a.

Turner, J., Maksym, T., Phillips, T., Marshall, G. J., and Meredith, M. P.: The impacts of changes in sea ice advance on the large winter warming on the western Antarctic Peninsula. Int. J. Climatol., 33, 852–861, doi:https://doi.org/10.1002/joc.3474, 2013b.

Wang, H., Rasch, P. J., Easter, R. C., Singh, B., Zhang, R., Ma, P.-L., Qian, Y., Ghan, S. J., and Beagley, N. Using an explicit emission tagging method in global modeling of source-receptor relationships for black carbon in the Arctic: Variations, sources, and transport pathways. J. Geophys. Res. Atmosphere, 119, 12888–12909, 2014.

Weijer, W., Veneziani, M., Stössel, A., Hecht, M. W., Jeffery, N., Jonko, A., Hodos, T., and Wang, H.: Local atmospheric response to an open-ocean polynya in a high-resolution climate model. J. Climate, 30, 1629–1641, https://doi.org/10.1175/JCLI-D-16-0120.1, 2017.

Winkelmann, R., Levermann, A., Martin, M. A., and Frieler, K.: Increased future ice discharge from Antarctica owing to higher snowfall, Nature, 492, 239–242, doi:10.1038/nature11616, 2012.

Zwally, H.J., Li, J., Robbins, J.W., Saba, J.L., Yi, D., Brenner, A.C. and Zwally, C.H.J.: Mass gains of the Antarctic ice sheet exceed losses. J. Glaciol, 61, 1019-1036, 2015.

https://doi.org/10.5194/tc-2019-69
Preprint. Discussion started: 12 June 2019

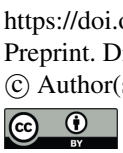

The Cryosphere
Discussions
Open Access
EGU

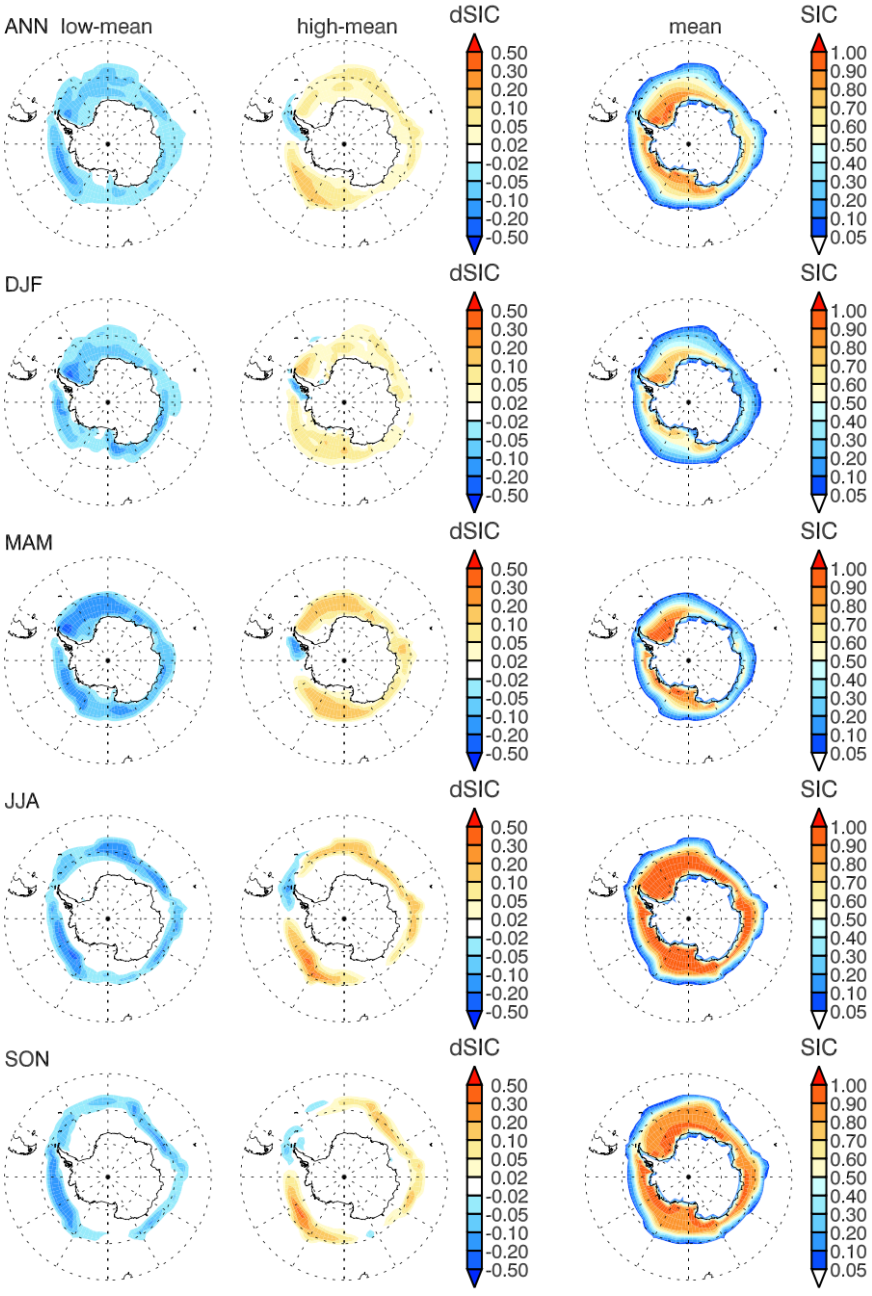

Figure 1: the anomalies of the two SIC composites ("low" and "high") with respect to the annual and seasonal mean SIC ("mean" in the right-most column).

https://doi.org/10.5194/tc-2019-69
Preprint. Discussion started: 12 June 2019

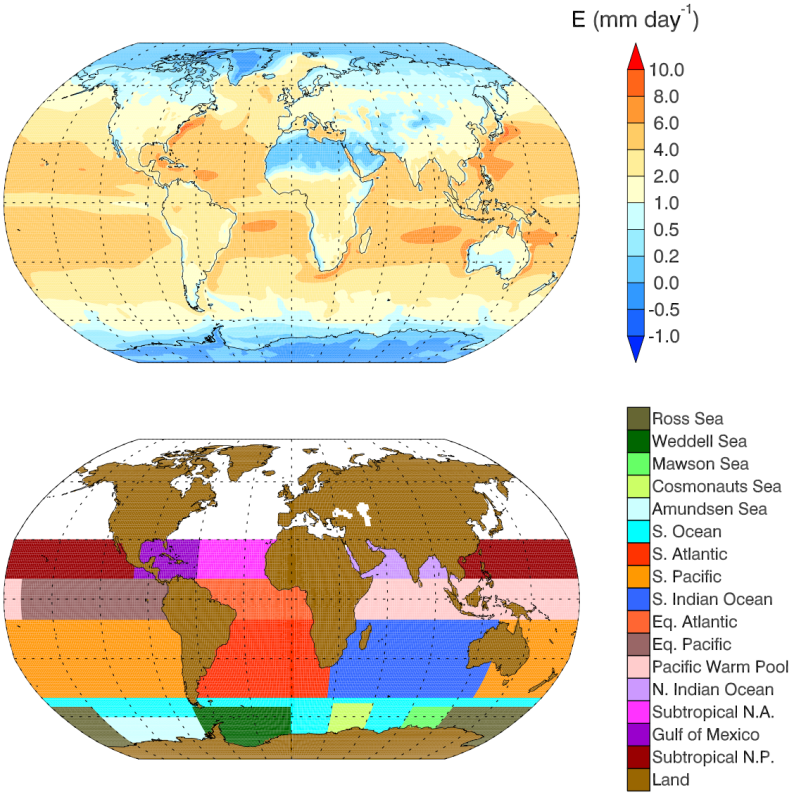

Figure 2: (top) Annual mean net evaporation/sublimation (positive values) at the surface. (bottom) Tagged water source regions that are potentially important for Antarctic precipitation, including all major tropical/subtropical and mid-latitude ocean basins (Subtropical N. Pacific, Subtropical N. Atlantic, Gulf of Mexico, Pacific Warm Pool, Equatorial Pacific, Equatorial Atlantic, N. Indian Ocean, S. Indian Ocean, S. Pacific, S. Atlantic, and S. Ocean), five finer sectors (Amundsen Sea, Cosmonauts Sea, Mawson Sea, Weddell Sea, and Ross Sea) in the Southern Ocean, and land (all continents). All remaining oceanic areas (white) are also tagged.

https://doi.org/10.5194/tc-2019-69
Preprint. Discussion started: 12 June 2019

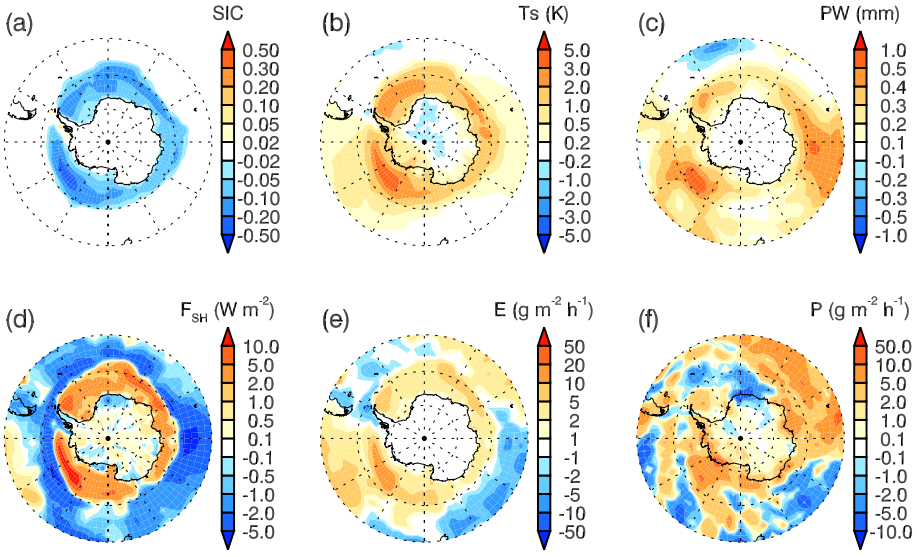

Figure 3: Annual mean differences in (a) sea ice concentrations (SIC), (b) surface temperature (Ts), (c) total precipitable water (PW), (d) surface sensible heat flux (F_{sh}), (e) surface evaporation/sublimation (E), (f) surface precipitation (P) between the "low" and "high" SIC cases.

https://doi.org/10.5194/tc-2019-69
Preprint. Discussion started: 12 June 2019

The Cryosphere
Discussions
Open Access
EGU

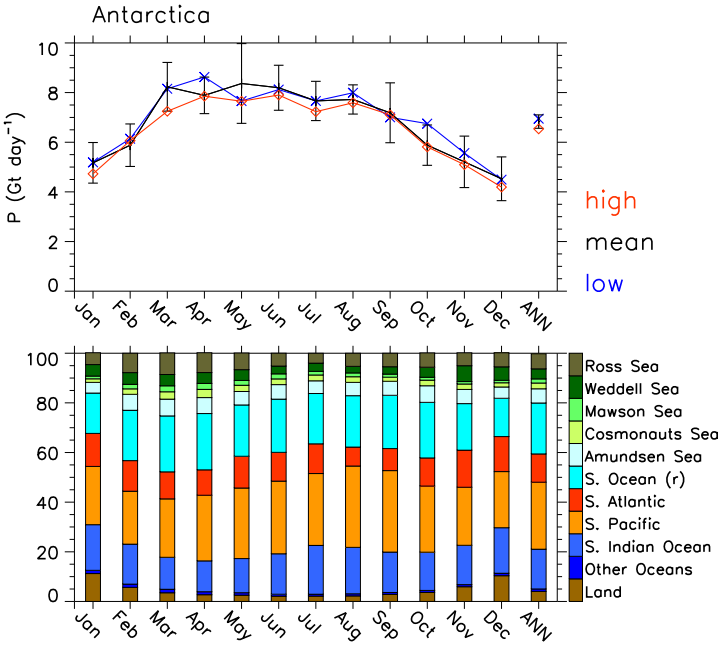

Figure 4: seasonal variation (January-December) and annual mean (ANN) precipitation over Antarctica in the three simulations (top) and the corresponding fractional contributions by the tagged source regions from the "mean" (bottom). Error bars represent one standard deviation of corresponding results from 10 individual years of the "mean" case. Note that the S. Ocean (r) tag plus the five sub-sector tags represent the entire Southern Ocean. Contributions from tropical oceans and northern hemisphere oceans are combined to the "Other Oceans".

https://doi.org/10.5194/tc-2019-69
Preprint. Discussion started: 12 June 2019

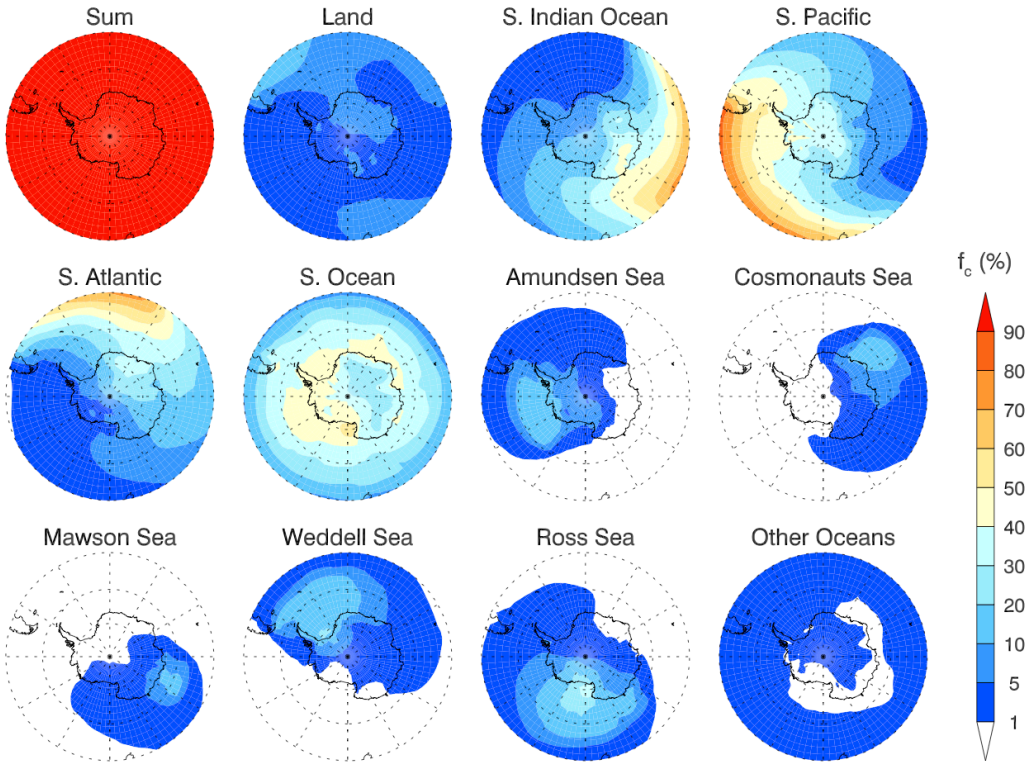

Figure 5: Spatial distribution of fractional contribution (%) to annual mean precipitation at the surface from individual source regions in the "mean" case. The "Sum" (upper-left panel) represents contributions from the five major source regions, including Land, S. Indian Ocean, S. Pacific, S. Atlantic and S. Ocean. Contributions from tropical oceans and northern hemisphere oceans are combined to the "Other Oceans".

https://doi.org/10.5194/tc-2019-69
Preprint. Discussion started: 12 June 2019

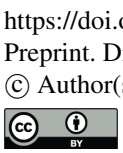

The Cryosphere
Discussions
Open Access
EGU

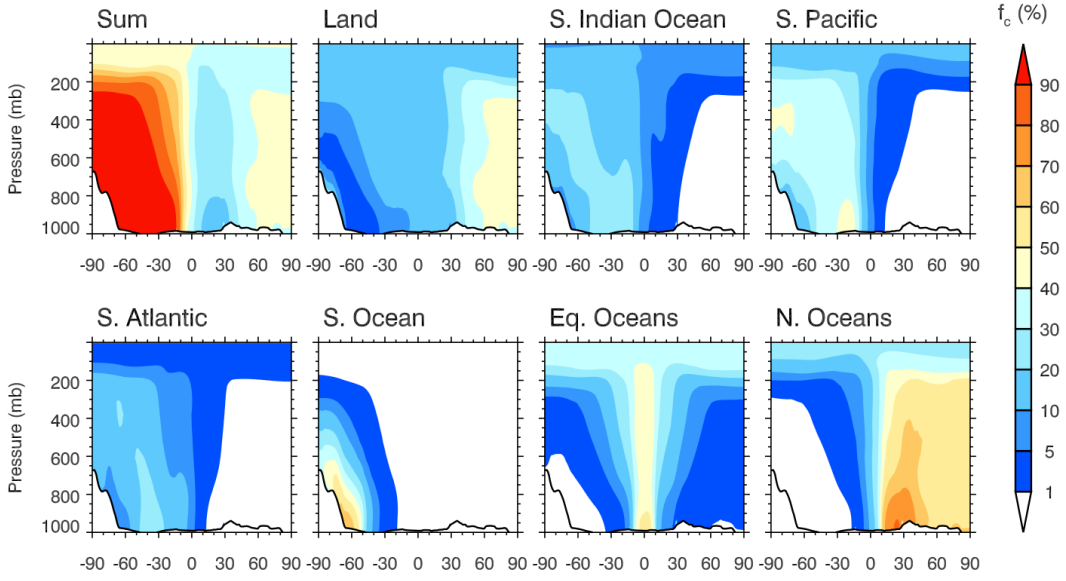

Figure 6: Vertical distribution of fractional contribution (%) to annual and zonal mean water vapor mixing ratio from individual source regions in the "mean" case. The "Sum" (upper-left panel) represents contributions from the five major source regions, including Land, S. Indian Ocean, S. Pacific, S. Atlantic and S. Ocean. The S. Ocean tag here includes all six sub-sectors. The Eq. Oceans includes the three equatorial ocean tags, and the N. Oceans includes the remaining ocean tags in the northern hemisphere.

https://doi.org/10.5194/tc-2019-69
Preprint. Discussion started: 12 June 2019

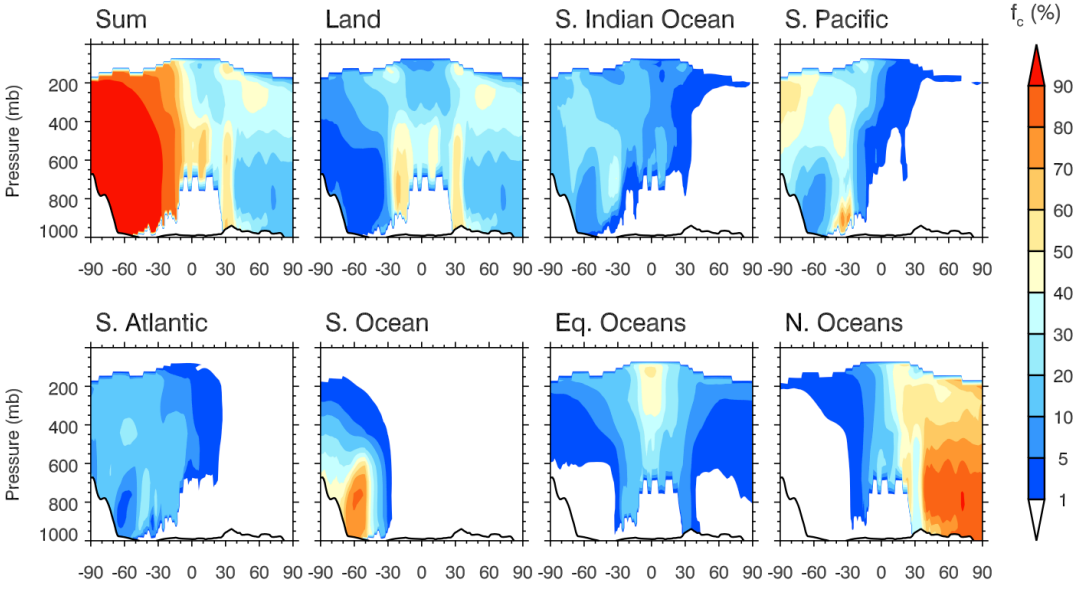

Figure 7: Same as Fig. 6 but for fractional contributions to zonal mean ice water mixing ratio.

https://doi.org/10.5194/tc-2019-69
Preprint. Discussion started: 12 June 2019

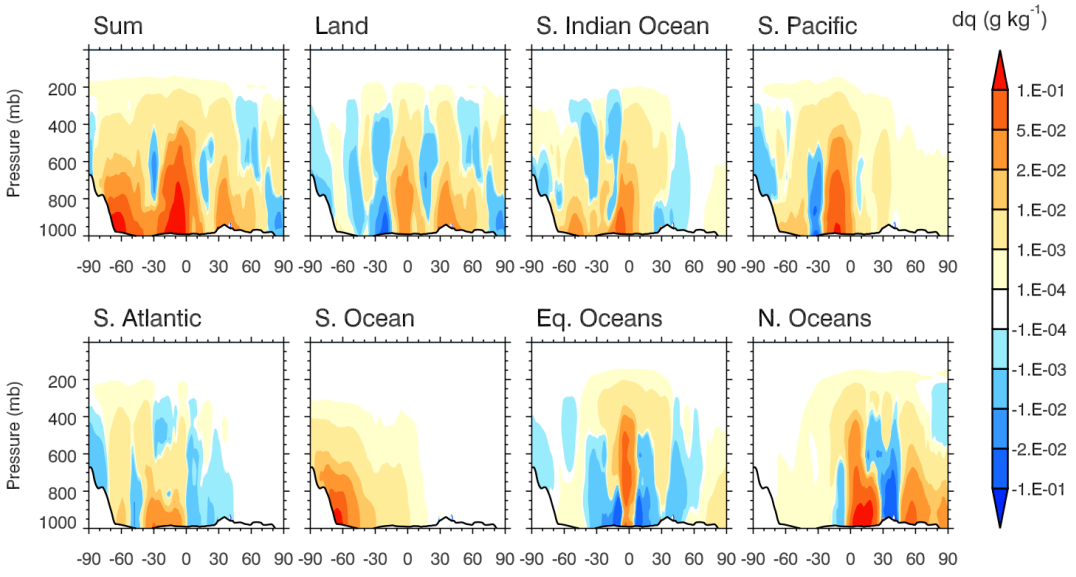

Figure 8: Vertical distribution of differences in annual and zonal mean water vapor mixing ratio between the "low" and "high" SIC cases. Note that the contour intervals are non-uniform.

https://doi.org/10.5194/tc-2019-69
Preprint. Discussion started: 12 June 2019

The Cryosphere
Discussions
Open Access
EGU

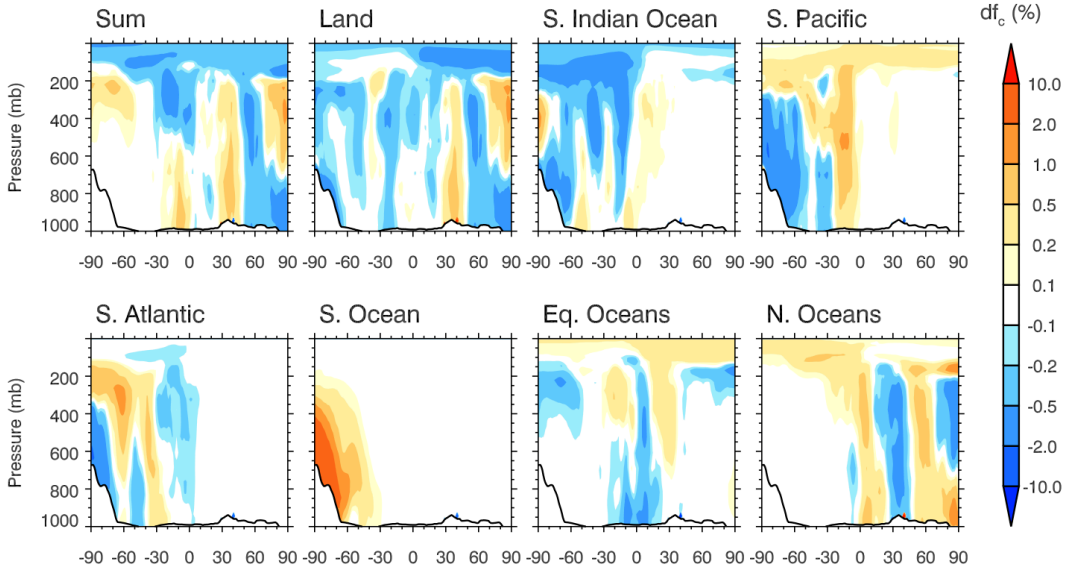

Figure 9: Same as Fig. 8 but for differences in fractional contribution to annual and zonal mean water vapor mixing ratio between the "low" and "high" SIC cases. Note that the contour intervals are non-uniform.

https://doi.org/10.5194/tc-2019-69
Preprint. Discussion started: 12 June 2019

The Cryosphere
Discussions
Open Access
EGU

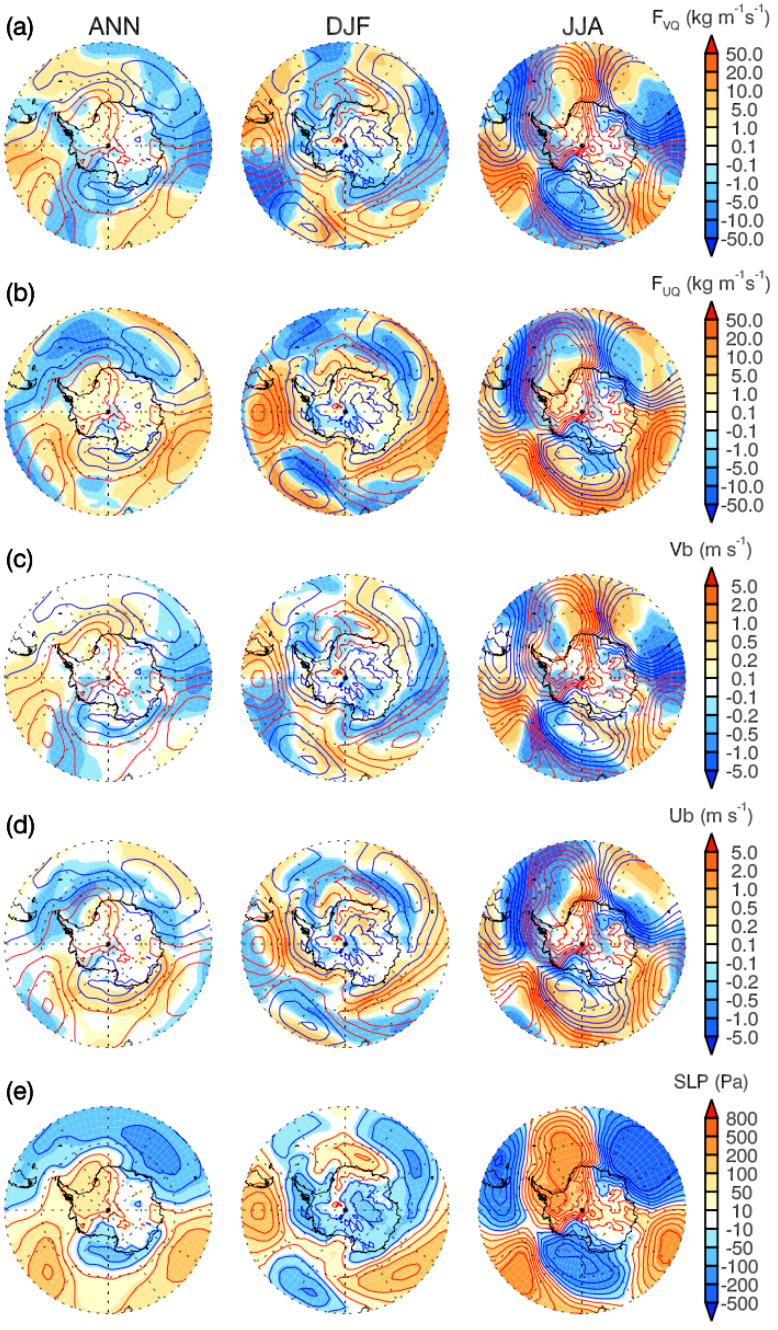

Figure 10: Spatial distribution of differences ("low" minus "high") in annual (left) and seasonal (DJF and JJA) mean column-integrated (a) meridional and (b) zonal moisture flux, (c) meridional and (c) zonal bottom-layer wind, and (e) sea level pressure (SLP). The superimposed contour lines represent SLP differences (red for positive and blue for negative; 40-Pa intervals).